Absence of superconductivity in the high-pressure polymorph of MgB_2

Yanming Ma,[1,2,*] Yanchao Wang,[1] and Artem R. Oganov[2,3]
[1]*National Lab of Superhard Materials, Jilin University, Changchun 130012, People's Republic of China*
[2]*Laboratory of Crystallography, Department of Materials, ETH Zurich, Wolfgang-Pauli-Stress 10, CH-8093 Zurich, Switzerland*
[3]*Geology Department, Moscow State University, 119992 Moscow, Russia*
(Received 22 October 2008; revised manuscript received 8 January 2009; published 2 February 2009)

We report a high-pressure orthorhombic KHg_2-type polymorph (space group *Imma*, 4 f.u./cell) of MgB_2 stable above 190 GPa predicted through *ab-initio* evolutionary simulations. The formation of this new phase results from the strong out-of-plane distortions of the two-dimensional honeycomb boron sublattice of the low-pressure AlB_2-type structure creating a peculiar tetrahedrally bonded three-dimensional boron network. This high-pressure phase is a weak metal and not superconducting, re-highlighting the key role of the planar boron sublattice in forming the superconducting state and clear structure-property relations that can enable design of new superconductors.

DOI: 10.1103/PhysRevB.79.054101 PACS number(s): 74.70.Ad, 61.50.Ks, 62.50.−p

At ambient pressure, the superconducting MgB_2 (Ref. 1) crystallizes in the AlB_2-type hexagonal structure (space group $P6/mmm$), in which B atoms form two-dimensional (2D) honeycomb layers, and Mg atoms sit above the centers of the hexagons in between the B planes. Within the B layer, each B atom forms three σ bonds (sp_xp_y hybridization), while a nonbonding π (p_z) wave function is localized above and below the B plane. The superconductivity of MgB_2 in this hexagonal structure arises mainly from the strong coupling between the in-plane E_{2g} phonon mode and the σ bonding states,[2–6] and the peculiar two-band superconducting nature[5,7] has fundamentally raised the transition temperature to be ~40 K.

Pressure could effectively shorten the interatomic distance of materials, and thus significantly alter their electronic bonding states to modify the physical properties and/or induce the formation of new physical states. Indeed, experiments demonstrated that the superconducting transition temperature (T_c) of MgB_2 decreases under pressure at a rate from −0.8 to −2.0 K/GPa (for example, see Refs. 8–12). This occurs continuously within the same structure and experimental measurements[11,13–16] up to 57 GPa did not reveal any structural phase transitions. Later, Loa *et al.*[17] and Shao *et al.*[18] suggested that if the applied pressure is high enough, an isosymmetric transition to the UHg_2-type structure might be possible since AlB_2 and UHg_2 are isopointal structures, distinguished only by their c/a ratios. However, our *ab-initio* calculations[19] ruled out this transition since the optimized c/a value of 1.15 at zero pressure decrease only slightly to 0.99 at 200 GPa, which is still well above the characteristic c/a of 0.60–0.85 for UHg_2. Therefore, the high-pressure phase of MgB_2 remains unknown. The discovery of new stable crystal forms of MgB_2 is of great fundamental interest and, in particular, would help to unravel the key factors responsible for the formation of superconducting states—a knowledge that can even be used for design of new high-T_c materials. In this paper, we have unraveled a high-pressure orthorhombic KHg_2-type structure of MgB_2 stable above 190 GPa and containing three-dimensional (3D) framework of B atoms, allowing us to re-highlight the major role of B-B π-bonded networks and charge transfer from metal atoms to B in the superconductivity.

Ab-initio evolutionary algorithm employed here was designed to search for the structure possessing the lowest free energy at given P/T conditions. The significant feature of this methodology is the capability of predicting the stable structure with only the knowledge of the chemical composition. The details of the search algorithm have been described elsewhere.[20–23] The evolutionary search was done with the USPEX code,[20–22] the underlying *ab-initio* structure relaxations were performed using density-functional theory (DFT) within the generalized gradient approximation (GGA) (Ref. 24) as implemented in the Vienna *ab-initio* simulation package (VASP) code.[25] The all-electron projector-augmented wave (PAW) (Refs. 26 and 27) method was adopted with the choices of $1s^2$ cores both for Mg and B atoms. We used the plane-wave kinetic-energy cutoff of 400 eV which was shown to give excellent convergence of the total energies and structural parameters. Electron-phonon coupling (EPC) has been explored using the pseudopotential plane-wave method and density-functional perturbation theory[28,29] as implemented in the QUANTUM-ESPRESSO package.[30] A Troullier-Martins (TM) (Ref. 31) norm-conserving scheme was used to generate pseudopotentials for Mg and B with the choices of electronic configurations of $2p^63s^2$ and $2s^22p^1$, respectively. In these calculations we used a kinetic-energy cutoff of 60 Ry and a $8\times6\times6$ Monkhorst-Pack (MP) grid, for which tests showed excellent convergence of the computed properties. The technique for the calculation of EPC has been described in detail in our previous publication.[32] Theoretical pressures are derived from the average of the diagonal components of the stress tensor in fine structural optimizations and confirmed by fitting the energy vs volume data to the Murnaghan equation of states. The use of TM or PAW method only affects slightly the theoretical pressures at the chosen volumes.

The variable-cell structure predictions were performed at 0, 100, 150, 200, 300, and 500 GPa with systems containing 3, 6, 9, 12, and 18 atoms in the simulation cell. At 0, 100, and 150 GPa, our simulations with the only input of chemical compositions of Mg:B=1:2 predicted the most stable structure to be AlB_2 type [Fig. 1(c)], in complete agreement with experiment. This successful prediction encourages us to explore higher-pressure phases. Our evolutionary simulations

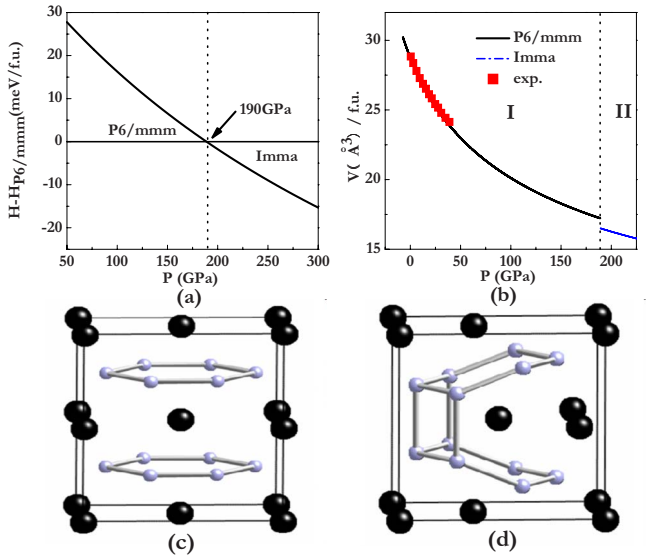

FIG. 1. (Color online) (a) Enthalpy of the KHg_2 structure (relative to AlB_2) with pressure. We used the $12\times12\times12$ and $8\times8\times8$ k meshes for AlB_2 and KHg_2, respectively, for which total energies are converged to be better than ~1 meV. (b) The calculated equations of state for the AlB_2 and KHg_2 phases, together with the experimental data from Ref. 16 for the AlB_2 phase. [(c) and (d)] Crystal structures of AlB_2 and KHg_2 phases, respectively. At 200 GPa for KHg_2 phase, lattice parameters: a=4.749 Å, b=2.855 Å, and c=4.795 Å; atomic positions: B at 8i (0.1817, 0.25, 0.5906) and Mg at 4e (0, 0.25, 0.1876).

at 200, 300, and 500 GPa identified a new stable orthorhombic *Imma* structure (4 f.u./cell) [Fig. 1(d)]. This structure is analogous to that of intermetallic compound KHg_2.[33] We have computed the full phonon-dispersion curves at 260 and 500 GPa and found no imaginary phonon frequencies, i.e., this structure is dynamically stable. The calculated enthalpies [Fig. 1(a)] show that the predicted new structure is thermodynamically stable above 190 GPa, where the current experimental techniques are readily accessible.

Our calculations suggest that the $AlB_2 \rightarrow KHg_2$ structural transition is first order and is accompanied by a pronounced 4.5% volume drop [Fig. 1(b)] and an increase in connectivity in the B framework from 3 to 4 [Fig. 1(c) and 1(d)]. This transition is in many ways similar to the graphite-diamond transition: graphitelike B lattice of the AlB_2 structure [Fig. 1(c)] transforms into a 3D network [Fig. 1(d)] resembling diamond (or the hexagonal diamond). The formation of KHg_2 structure can be imaged to result from a strong out-of-plane distortion of the honeycomb B sublattice and concomitant displacements of the Mg atoms. As a result, B atoms form a strongly puckered network of tilted hexagons and the Mg atoms lie between opposite hexagons. At the transition, the number of nearest neighbors increases from 3 to 1+2+1, and the B-B distances increase from 1.561 Å in parent planar hexagons to 1.661/1.671 Å in the tilted hexagons of the child KHg_2 structure. The newly formed fourth covalent B-B bond between the hexagons (its length is 1.726 Å) is confirmed by the deformation electron-density plots.

Energy bands for KHg_2 structure at 200 GPa are shown in Fig. 2 to illustrate the electronic properties of the high-pressure polymorph. A weak band overlap implies this is a poor metal with a very small electronic density of states (DOS) at the Fermi level (N_0) [Fig. 3(c)]. 3D Fermi-surface pieces [Fig. 2(c)] are found to be mainly located along the

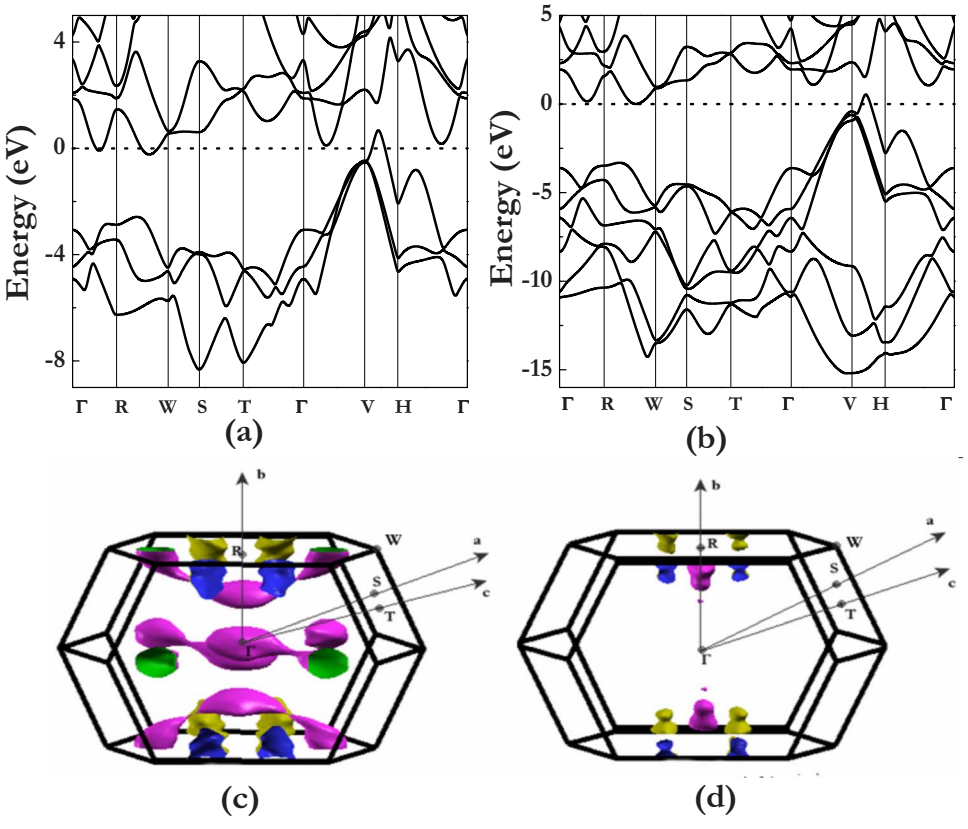

FIG. 2. (Color online) Band structures for the KHg_2 phase at (a) 200 GPa and (b) 500 GPa. Low-symmetry special k-points V (−0.49523, 0.49523, 0.49523) and H (−0.33385, 0.33385, 0.6566) had to be chosen to reveal band overlap. 3D Fermi-surface plots for the KHg_2 structure at (c) 200 GPa and (d) 500 GPa. Note that at 200 GPa, Γ point is located in between two Fermi-surface pockets.

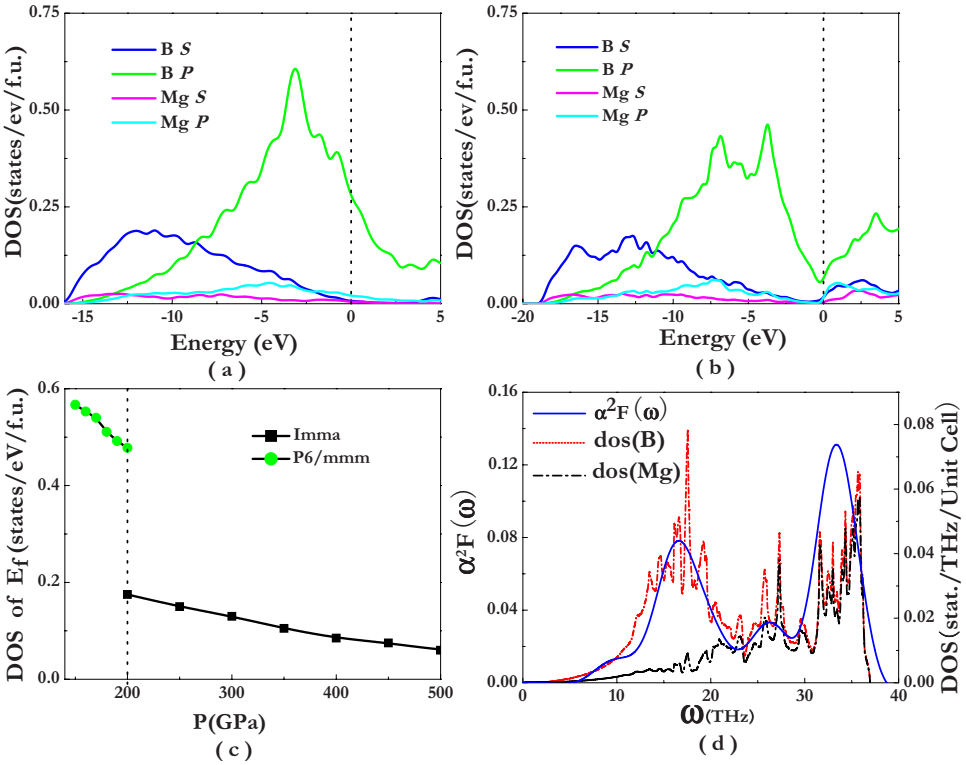

FIG. 3. (Color online) Partial electronic DOS at 200 GPa for (a) AlB_2 and (b) KHg_2 structures. (c) Electronic DOS at Fermi level for AlB_2 (solid circles) and KHg_2 (solid squares) structures. (d) The calculated projected phonon DOS and EPC spectral function $\alpha^2F(\omega)$ for the KHg_2 structure at 200 GPa.

low-symmetry lines in the first Brillouin zone (BZ). Intriguingly, with increasing pressure, the bottom of the conduction band along Γ-R-W and Γ-V directions shifts above the Fermi level [Fig. 2(b)], causing N_0 to decrease with pressure [Fig. 3(c)]. The significant changes in the Fermi-surface profiles [Fig. 2(d)] will inevitably induce an electronic topological transition (ETT). However, the ETT does not affect the KHg_2 structure, as suggested by the continuous changes in lattice parameters with pressure. It is known that DFT usually underestimates the band gap. GW calculations[34,35] (known to provide accurate description of band gaps, within 10% of the experimental values[36]) were thus adopted to carefully confirm the metallicity of KHg_2 phase at 200 GPa. Particular care was paid to the energy values of the eighth band (highest valence band) and the ninth band (lowest conduction band) with respect to the Fermi energy. It turns out that with the GW correction, the ninth band moves above Fermi level, but the eighth band still crosses over the Fermi level. The metallic feature remains. Note that the GW calculation is only at an attempt to correct the band energies in assessment of the metallicity, but other results (e.g., electronic DOS, Fermi surfaces, phonons, and EPC) are not corrected.

Inspection of the electronic DOSs of the AlB_2 and KHg_2 phases [Fig. 3(a) and 3(b)] suggests that p electrons of B atoms dominate the electronic behavior at the Fermi level. Therefore, it is essential to understand how the B framework is modified in order to uncover the physical origin of the N_0 drop at the transition [Fig. 3(c)]. In the AlB_2 phase, each B atom has three valence electrons that are used to form three coplanar σ bonds (sp^2 hybridization). Under pressure, four B-B σ bonds (sp^3 hybridization) are constructed for the KHg_2 phase. Note that four B-N covalent bonds are known earlier in cubic/wurtzite BN, where each B atom contributes 0.75 electrons to the B-N bond. However, the formation of four tetrahedral B-B covalent bonds is very unusual for any B-related materials. At the transition, the charge density localized at the three B-B bonds in the honeycomb lattice is depleted in order to allow the formation of the fourth bond between hexagons, consistent with the increase in the B-B distance. The resulting 3D framework lacks the system of π bonds with mobile electrons and has more localized electrons, as a result of which the conductivity drops.

The projected phonon DOSs and the EPC spectral function $\alpha^2F(\omega)$ for KHg_2 structure at 200 GPa have been presented in Fig. 3(d). It is found that all the phonons contribute to the EPC, signifying an isotropic EPC feature originated from the 3D structural nature. This is in apparent contrast with the strongly anisotropic EPC behavior in AlB_2 structure. The obtained EPC λ for KHg_2 phase at 200 GPa is 0.11, which is very small and has a zero T_c. To eliminate the pressure effect on the EPC of KHg_2 structure in view of the greatly depressed T_c in AlB_2 structure, we optimized the KHg_2 structure to zero pressure and performed the EPC calculations. Again, the resulting λ value is very small, 0.24 ($T_c = \sim 0$ K). Therefore, we conclude that KHg_2-type MgB_2 is intrinsically not a good superconductor. The current calculations have confirmed that instead of materials compositions, the crystal structure is the dominant factor for superconductivity. Here, the B-layered structure is advantageous for high T_c.

The most fruitful and intuitive way to understand the electronic and structural properties of MgB_2 is to invoke its profound analogy with carbon. Graphite, in which carbon prefers the sp^2 hybridization, is an ambient pressure form of carbon with a zero band gap. Under sufficient compression, graphite transforms to diamond—a wide-gap insulator characterized by sp^3 hybridization. To be isoelectronic with carbon, B atom misses one electron. In MgB_2 this one missing

electron is donated by Mg atoms. If charge transfers were complete, the low-pressure hexagonal form would have (like graphite) a zero band gap, and the KHg_2 phase would be a wide-gap insulator (removing Mg from the KHg_2 structure and replacing B with C, after full structural optimization we see an insulating structure similar to hexagonal diamond). A consequence of incomplete charge transfer (as in MgB_2) is a finite DOS at the Fermi level (i.e., metallic character) and hole conductivity, as shown in Fig. 2. Mulliken population analysis suggests an increase in charge transfer from Mg to B at a rate of 4×10^{-3} e/GPa; this naturally leads to a decrease in N_0 (and T_c for the AlB_2 phase) with increasing pressure [Fig. 3(c)]. These observations allow us to identify two key factors for superconductivity in MgB_2 and related borides. First, geometry and bonding in the B sublattice (graphite vs diamond, networks of delocalized π bonds vs frameworks of localized σ bonds) are crucial. Second, as the amount of charge transfer (which determines the DOS at the Fermi level) depends on the electronegativity of the cation, we identify electronegativity of the donor atom as an important factor governing T_c. The first rule draws our attention to graphitelike (e.g., MgB_2 in the AlB_2 form) and fullerenelike (materials with B_{12} icosahedra) structures with systems of delocalized π bonds (we note that for carbon, doped graphite and especially fullerenes are superconductors), while the second suggests a hole doping or replacing Mg with more electronegative cations (e.g., Be).[37]

Previously, Singh[38] has proposed a pressure-induced B_{1g} mode softening in AlB_2 structure at 143 GPa by employing the semi-empirical lattice parameters. However, our calculations in use of the lattice data by *ab-initio* structural optimization do not support this.[19] In fact, all phonon frequencies were found to increase with pressure up to the transition pressure of 190 GPa. We thus eliminate phonon softening as the driving force for the structural transition. Nevertheless, in view of the electronic DOS in KHg_2 structure [Fig. 3(b)], it is suggested that a well-defined electronic pseudogap might effectively lower the total energy and, together with its higher density, stabilize the new phase.

In summary, we have first reported a high-pressure KHg_2-type crystal form of MgB_2 found using the recently developed *ab-initio* evolutionary algorithm. This structure possesses an intriguing sp^3 B-B bonded network and displays a semimetallic behavior. The superconducting state is destroyed with the formation of this 3D B lattice. Our predictions re-highlight the major role of B-B π-bonded networks and charge transfer from metal atoms to boron. These ideas are useful for the design of novel superconductors.

Y.M. and Y.W. are thankful for the partial financial support from the China 973 Program under Grant No. 2005CB724400, the National Natural Science Foundation of China under Grant No. 10874054, the NSAF of China under Grant No. 10676011, and the 2007 Cheung Kong Scholars Programme of China. Y.M. and A.R.O. gratefully acknowledge financial support from the Swiss National Science Foundation under Grant No. 200021-111847/1.

*Corresponding author: mym@jlu.edu.cn

[1] J. Nagamatsu, N. Nakagawa, T. Muranaka, Y. Zenitani, and J. Akimitsu, Nature (London) **410**, 63 (2001).
[2] K. P. Bohnen, R. Heid, and B. Renker, Phys. Rev. Lett. **86**, 5771 (2001).
[3] Y. Kong, O. V. Dolgov, O. Jepsen, and O. K. Andersen, Phys. Rev. B **64**, 020501(R) (2001).
[4] M. Iavarone, G. Karapetrov, A. E. Koshelev, W. K. Kwok, G. W. Crabtree, D. G. Hinks, W. N. Kang, Eun-Mi Choi, Hyun Jung Kim, Hyeong-Jin Kim, and S. I. Lee, Phys. Rev. Lett. **89**, 187002 (2002).
[5] H. J. Choi, D. Roundy, H. Sun, M. L. Cohen, and S. G. Louie, Nature (London) **418**, 758 (2002).
[6] T. Yildirim, O. Gülseren, J. W. Lynn, C. M. Brown, T. J. Udovic, Q. Huang, N. Rogado, K. A. Regan, M. A. Hayward, J. S. Slusky, T. He, M. K. Haas, P. Khalifah, K. Inumaru, and R. J. Cava, Phys. Rev. Lett. **87**, 037001 (2001).
[7] W. Pickett, Nature (London) **418**, 733 (2002).
[8] T. Tomita, J. J. Hamlin, J. S. Schilling, D. G. Hinks, and J. D. Jorgensen, Phys. Rev. B **64**, 092505 (2001).
[9] M. Monteverde, M. Nunez-Regueiro, N. Rogado, K. A. Regan, M. A. Hayward, T. He, S. M. Loureiro, and R. J. Cava, Science **292**, 75 (2001).
[10] S. Deemyad, T. Tomita, J. J. Hamlin, B. R. Beckett, J. S. Schilling, D. G. Hinks, J. D. Jorgensen, S. Lee, and S. Tajima, Physica C **385**, 105 (2003).
[11] J. Tang, L. C. Qin, A. Matsushita, Y. Takano, K. Togano, H. Kito, and H. Ihara, Phys. Rev. B **64**, 132509 (2001).
[12] B. Lorenz, R. L. Meng, and C. W. Chu, Phys. Rev. B **64**, 012507 (2001).
[13] A. F. Goncharov, V. V. Struzhkin, E. Gregoryanz, J. Z. Hu, R. J. Hemley, H. K. Mao, G. Lapertot, S. L. Bud'ko, and P. C. Canfield, Phys. Rev. B **64**, 100509(R) (2001).
[14] J. D. Jorgensen, D. G. Hinks, and S. Short, Phys. Rev. B **63**, 224522 (2001).
[15] J. Tang, L. C. Qin, H. W. Gu, A. Matsushita, Y. Takano, K. Togano, H. Kito, and H. Ihara, J. Phys.: Condens. Matter **14**, 10623 (2002).
[16] P. Bordet, M. Mezouar, M. Núñez-Regueiro, M. Monteverde, M. D. Núñez-Regueiro, N. Rogado, K. A. Regan, M. A. Hayward, T. He, S. M. Loureiro, and R. J. Cava, Phys. Rev. B **64**, 172502 (2001).
[17] I. Loa, K. Kunc, K. Syassen, and P. Bouvier, Phys. Rev. B **66**, 134101 (2002).
[18] Y. Shao and X. Zhang, J. Phys.: Condens. Matter **16**, 1103 (2004).
[19] Y. Wang and Y. Ma (unpublished).
[20] A. R. Oganov and C. W. Glass, J. Chem. Phys. **124**, 244704 (2006).
[21] A. R. Oganov, C. W. Glass, and S. Ono, Earth Planet. Sci. Lett. **241**, 95 (2006).
[22] C. W. Glass, A. R. Oganov, and N. Hansen, Comput. Phys. Com-

mun. **175**, 713 (2006).
[23] Y. M. Ma, A. R. Oganov, and C. W. Glass, Phys. Rev. B **76**, 064101 (2007).
[24] J. P. Perdew, K. Burke, and M. Ernzerhof, Phys. Rev. Lett. **77**, 3865 (1996).
[25] G. Kresse and J. Furthmuller, Phys. Rev. B **54**, 11169 (1996).
[26] G. Kresse and D. Joubert, Phys. Rev. B **59**, 1758 (1999).
[27] P. E. Blochl, Phys. Rev. B **50**, 17953 (1994).
[28] S. Baroni, P. Giannozzi, and A. Testa, Phys. Rev. Lett. **58**, 1861 (1987).
[29] P. Giannozzi, S. de Gironcoli, P. Pavone, and S. Baroni, Phys. Rev. B **43**, 7231 (1991).
[30] A. D. C. S. Baroni, S. de Gironcoli, P. Giannozzi, C. Cavazzoni, G. Ballabio, S. Scandolo, G. Chiarotti, P. Focher, A. Pasquarello, K. Laasonen, A. Trave, R. Car, N. Marzari, and A. Kokalj, http://www.pwscf.org
[31] N. Troullier and J. L. Martins, Phys. Rev. B **43**, 1993 (1991).
[32] Y. M. Ma, J. S. Tse, D. D. Klug, and R. Ahuja, Phys. Rev. B **70**, 214107 (2004).
[33] E. J. Duwell and N. C. Baenziger, Acta Crystallogr. **8**, 705 (1955).
[34] M. S. Hybertsen and S. G. Louie, Phys. Rev. B **34**, 5390 (1986).
[35] X. Gonze, *et al.*, Comput. Mater. Sci. **25**, 478 (2002).
[36] M. Shishkin and G. Kresse, Phys. Rev. B **75**, 235102 (2007).
[37] In order to demonstrate our idea, we have performed EPC calculations for BeB2 within AlB2 structure. We use Be pseudopotential but adopt the atomic mass of Mg to better compare with MgB2. At zero pressure, the resulting λ for BeB2 is 0.89, much larger than that (0.73) of MgB2. Note that the two EPC calculations for BeB2 and MgB2 are performed at nearly identical conditions to have a good comparison.
[38] P. P. Singh, Phys. Rev. Lett. **97**, 247002 (2006).